Simulating Changes in Regional Air Pollution over the Eastern United States Due to Changes in Global and Regional Climate and Emissions

Simulating changes in regional air pollution over the eastern United States due to changes in global and regional climate and emissions

C. Hogrefe,[1] B. Lynn,[2] K. Civerolo,[3] J.-Y. Ku,[3] J. Rosenthal,[4] C. Rosenzweig,[5] R. Goldberg,[5] S. Gaffin,[2] K. Knowlton,[4] and P. L. Kinney[4]

Received 25 February 2004; revised 23 July 2004; accepted 13 September 2004; published 17 November 2004.

[1] To simulate ozone (O_3) air quality in future decades over the eastern United States, a modeling system consisting of the NASA Goddard Institute for Space Studies Atmosphere-Ocean Global Climate Model, the Pennsylvania State University/National Center for Atmospheric Research mesoscale regional climate model (MM5), and the Community Multiscale Air Quality model has been applied. Estimates of future emissions of greenhouse gases and ozone precursors are based on the A2 scenario developed by the Intergovernmental Panel on Climate Change (IPCC), one of the scenarios with the highest growth of CO_2 among all IPCC scenarios. Simulation results for five summers in the 2020s, 2050s, and 2080s indicate that summertime average daily maximum 8-hour O_3 concentrations increase by 2.7, 4.2, and 5.0 ppb, respectively, as a result of regional climate change alone with respect to five summers in the 1990s. Through additional sensitivity simulations for the five summers in the 2050s the relative impact of changes in regional climate, anthropogenic emissions within the modeling domain, and changed boundary conditions approximating possible changes of global atmospheric composition was investigated. Changed boundary conditions are found to be the largest contributor to changes in predicted summertime average daily maximum 8-hour O_3 concentrations (5.0 ppb), followed by the effects of regional climate change (4.2 ppb) and the effects of increased anthropogenic emissions (1.3 ppb). However, when changes in the fourth highest summertime 8-hour O_3 concentration are considered, changes in regional climate are the most important contributor to simulated concentration changes (7.6 ppb), followed by the effect of increased anthropogenic emissions (3.9 ppb) and increased boundary conditions (2.8 ppb). Thus, while previous studies have pointed out the potentially important contribution of growing global emissions and intercontinental transport to O_3 air quality in the United States for future decades, the results presented here imply that it may be equally important to consider the effects of a changing climate when planning for the future attainment of regional-scale air quality standards such as the U.S. national ambient air quality standard that is based on the fourth highest annual daily maximum 8-hour O_3 concentration. *INDEX TERMS:* 0345 Atmospheric Composition and Structure: Pollution—urban and regional (0305); 1610 Global Change: Atmosphere (0315, 0325); 1630 Global Change: Impact phenomena; 3309 Meteorology and Atmospheric Dynamics: Climatology (1620); *KEYWORDS:* air quality standards, ozone pollution, regional climate change impacts

Citation: Hogrefe, C., B. Lynn, K. Civerolo, J.-Y. Ku, J. Rosenthal, C. Rosenzweig, R. Goldberg, S. Gaffin, K. Knowlton, and P. L. Kinney (2004), Simulating changes in regional air pollution over the eastern United States due to changes in global and regional climate and emissions, *J. Geophys. Res.*, *109*, D22301, doi:10.1029/2004JD004690.

1. Introduction

[2] In recent years, there has been a growing realization that regional-scale ozone (O_3) air quality is influenced by processes occurring on global scales, such as the intercontinental transport of pollutants [*Jacob et al.*, 1999; *Fiore et al.*, 2002a, 2003a, 2003b; *Yienger et al.*, 2000; *Wild and Akimoto*, 2001; *Holloway et al.*, 2003] and the projected growth in global emissions that alter the chemical composition of the troposphere [*Prather and Ehhalt*, 2001; *Prather et al.*, 2003; *Fiore et al.*, 2002b]. There have also been several global-scale studies that investigated the po-

[1]Atmospheric Sciences Research Center, State University of New York at Albany, Albany, New York, USA.
[2]Center for Climate Systems Research, Columbia Earth Institute of Columbia University, Columbia University, New York, New York, USA.
[3]New York State Department of Environmental Conservation, Bureau of Air Quality Analysis and Research, Albany, New York, USA.
[4]Mailman School of Public Health, Columbia University, New York, New York, USA.
[5]NASA Goddard Institute for Space Studies, New York, New York, USA.

0148-0227/04/2004JD004690$09.00

tential impact of climate change on global tropospheric chemistry [*Brasseur et al.*, 1998; *Johnson et al.*, 1999, 2001]. However, modeling studies on urban and regional scales are needed to assess the potential public health impacts of climate change through the alteration of near-surface air pollution [*McCarthy et al.*, 2001]. Climate change can influence the concentration and distribution of air pollutants through a variety of direct and indirect processes, including the modification of biogenic emissions [*Constable et al.*, 1999], the change of chemical reaction rates, changes in mixed-layer heights that affect vertical mixing of pollutants, and modifications of synoptic flow patterns that govern pollutant transport. On the global scale, *Brasseur et al.* [1998] and *Johnson et al.* [1999, 2001] have shown that the increase of temperature and water vapor due to climate change would lead to a net decrease in total tropospheric O_3 concentrations. On the other hand, on the regional scale, warmer temperatures can result in an increase of near-surface O_3 concentrations in urban and polluted rural environments [*Sillman and Samson*, 1995]. *Aw and Kleeman* [2003] showed through simulations that interannual temperature variability can change peak O_3 concentrations by 16% when other meteorological variables and emissions patterns were held constant. Analysis of ozone observations also reveals the influence of meteorology on ambient ozone concentrations. For example, O_3 concentrations in the eastern United States during the summer of 2003 were lower than average, at least partially due to below-average temperatures and above-average rainfall during this period [*U.S. Environmental Protection Agency*, 2004].

[3] In this paper, results are presented for a modeling study aimed at simulating O_3 concentrations over the eastern United States in three future decades, taking into account the effects of regional climate change. Regional climate change was simulated by one-way coupling of a mesoscale meteorological model to a global climate model. This multicomponent approach enables the elucidation of the effects of climate change on regional and urban scales that could not be obtained from the global simulations. Additionally, the results of sensitivity simulations investigating the contribution of increased biogenic emissions to changed O_3 in the future climate are presented. Finally, additional sensitivity simulations were performed to compare O_3 changes due to regional climate change to those that could arise from changes in projected anthropogenic emissions within the modeling domain and changes in chemical boundary conditions approximating potential changes in global atmospheric composition.

2. Models and Database

[4] Projections of greenhouse gas and other atmospheric constituents are used as inputs to climate and air quality models to simulate possible future conditions. The Intergovernmental Panel on Climate Change Special Report on Emission Scenarios (SRES) describes various future emissions scenarios based on projections of population, technology change, economic growth, etc. [*Intergovernmental Panel on Climate Change* (*IPCC*), 2000]. In this paper we utilize the emission projections of the SRES A2 marker scenario generated by the Atmospheric Stabilization Framework socioeconomic model [*Pepper et al.*, 1998; *Sankovski et al.*, 2000]. This scenario is one of the more pessimistic SRES marker scenarios and is characterized by a large increase of CO_2 emissions, relatively weak environmental concerns, little convergence between regions, and a large population increase to 15 billion people by 2100 [*IPCC*, 2000].

2.1. Emissions Processing

[5] Because the SRES emission scenarios are global in nature, their spatial resolution is not adequate for regional air quality modeling. Therefore the county level U.S. Environmental Protection Agency (EPA) 1996 National Emissions Trends inventory is used as the basis for air quality modeling. This emission inventory is processed by the Sparse Matrix Operator Kernel Emissions Modeling System (SMOKE) (Carolina Environmental Programs, Sparse Matrix Operator Kernel Emission (SMOKE) modeling system, available from University of North Carolina's Carolina Environmental Program website at http://www.cep.unc.edu/empd/EDSS/emissions) to obtain gridded, hourly, speciated emission inputs for the air quality model. Mobile source emissions were estimated by the Mobile5b model [*U.S. Environmental Protection Agency*, 1994] integrated into SMOKE. Biogenic emissions were estimated by the biogenic emissions inventory system, version 2 (BEIS2) that takes into account the effects of temperature and solar radiation on the rates of these emissions [*Geron et al.*, 1994; *Williams et al.*, 1992]. Specifically, emission rates of isoprene, other volatile organic compounds (VOC), and NO are sensitive to changes in temperature in BEIS2. The same land use data set was used to calculate biogenic emissions for all simulations, i.e., the possible feedback of climate change on land use and vegetation cover was not considered in this study. NO_x formation by lightning and its sensitivity toward climate change were not included in the modeling system. For some of the sensitivity simulations described in section 2.3, future year anthropogenic emissions of VOC and NO_x are estimated by multiplying the 1996 base year emission inventory with the regional growth factors for the SRES A2 scenario for the so-called OECD90 region (all countries that belonged to the Organization for Economic Cooperative Development (OECD) as of 1990) that includes many industrialized countries including the United States. Changes in regional CO emissions were not considered in these simulations. The anthropogenic VOC and NO_x emissions for this scenario for 1995 (calculated as the average of 1990 and 2000), 2020, 2050, and 2080 are shown in Table 1 for both the OECD90 region and for the global total [*IPCC*, 2000]. Table 1 illustrates that the emissions of the O_3 precursors NO_x/VOC increase by 125/60% globally and 29/8% for the OECD90 region by the 2050s.

2.2. Global and Regional Climate Modeling

[6] Current and future year regional climate fields were obtained by coupling the Pennsylvania State University/National Center for Atmospheric Research mesoscale regional climate model (MM5) [*Grell et al.*, 1994] to the Goddard Institute for Space Studies (GISS) $4^\circ \times 5^\circ$ resolution Global Atmosphere-Ocean Model (GISS-GCM) [*Russell et al.*, 1995] in a one-way mode through initial

Table 1. Total Annual Global and OECD90 Anthropogenic VOC and NO_x Emissions for the A2 Scenario for 1995, 2020, 2050, and 2080[a]

	1995	2020	2050	2080
VOC-global, Mt	140.2	178.6	225.2	275.0
NO_x-global, Mt N	31.5	50.3	71.1	87.5
VOC-OECD90, Mt	39.2	44.4	42.3	50.0
NO_x-OECD90, Mt N	12.5	15.6	16.2	17.0

[a]Data are from *IPCC* [2000].

conditions and lateral boundaries. Six-hourly GISS-GCM temperature, wind, pressure, and moisture fields were interpolated to the lateral boundaries of the MM5 grid. A five-point linear time interpolation was used to make the lateral boundary data synchronous with the MM5 time steps, following *Davies and Turner* [1977]. Simulations were performed for five consecutive summer seasons (June–August) in the 1990s and three future decades, namely 1993–1997, 2023–2027, 2053–2057, and 2083–2087. The month of May was used for spin-up in each model simulation and not utilized for the air quality simulations. The MM5 was applied in a nested grid mode with an inner grid having a horizontal resolution of 36 km over the eastern United States and an outer grid having a horizontal resolution of 108 km covering most of the continental United States as illustrated in Figure 1; only results from the 36-km simulation were used to perform the air quality simulations. The MM5 had 35 vertical layers; the height of the first layer interface was ~70 m while the height of the first layer midpoint was ~35 m. B. H. Lynn et al. (The GISS-MM5 regional climate modeling system: part I: Sensitivity of simulated current and future climate to model configuration, submitted to *Journal of Climate*, 2004, hereinafter referred to as Lynn et al., submitted manuscript, 2004) tested several different combinations of MM5 physics options; in this study we selected the MM5 simulations that were performed with the Medium Range Forecast Model boundary layer scheme [*Hong and Pan*, 1996], the Betts-Miller cloud scheme [*Betts*, 1986], and the Rapid Radiation Transfer Model radiation scheme [*Mlawer et al.*, 1997]. Table 2 provides an overview of atmospheric CO_2 abundances for the A2 scenario [*IPCC*, 2001] and the temperature response of the GISS-GCM and MM5 models over all nonwater grid cells for the 36-km Community Multiscale Air Quality (CMAQ) modeling domain depicted in Figure 1. It can be seen that MM5 predicts larger temperature increases than the GISS-GCM; the difference increases from 0.2°C in the 2020s to 1.5°C in the 2080s. Both the temperature increases predicted by the GISS-CGM and MM5 are within the range of temperature changes predicted by other global climate models for the A2 scenario for the same region [*IPCC*, 2001]. Further details on the setup of this modeling system and results of the future regional climate simulations are described by Lynn et al. (submitted manuscript, 2004).

2.3. Air Quality Modeling

[7] Using the SMOKE-processed emissions and the 36-km MM5 regional climate simulations for the five summer seasons in the 1990s, 2020s, 2050s, and 2080s, air quality simulations were performed using the CMAQ model [*Byun and Ching*, 1999]. To minimize the effect of initial conditions, CMAQ predictions during the initial 3-day period of each model simulation were considered as spin-up and excluded from subsequent analysis. *Berge et al.* [2001] showed that for model simulations of oxidant chemistry the effects of local emissions patterns and meteorology dominate over the effects of initial conditions after a 3-day spin-up period and that initial conditions have a minimal impact on ozone simulation results after such a spin-up period. A 3-day spin-up period also has been utilized in several other regional-scale ozone modeling studies for the United States [*Sistla et al.*, 2001; *Tao et al.*, 2003]. The Carbon Bond IV Mechanism [*Gery et al.*, 1989] was used to simulate gas phase chemistry. The 36-km CMAQ modeling domain used in this study consists of 68 × 59 horizontal and 16 vertical grid cells and is depicted in Figure 1. This domain represents a slightly reduced subgrid of the full 36-km MM5 modeling domain. The same Lambert-Conformal map projection and σ_p vertical coordinate system was used in MM5 and CMAQ, eliminating the need for horizontal or vertical interpolation of the meteorological fields. However, the vertical resolution of the CMAQ grid was reduced from that of the MM5 grid through the use of layer-collapsing for layers above 3 km. Also depicted in Figure 1 are the locations of 428 O_3 monitors from the U.S. EPA's Air Quality System (http://www.epa.gov/air/data/aqsdb.html) within the modeling domain. For some of the analyses presented in sections 3.1–3.3, results are spatially averaged over these monitors to investigate the effects of climate change at locations that are chosen to monitor the public health impacts of O_3 concentrations.

[8] The CMAQ model has undergone extensive community development and peer review and has been used successfully for a number of regional air quality studies [*Ku et al.*, 2001; *Mebust et al.*, 2003; *Bell and Ellis*, 2003; *Hogrefe et al.*, 2004]. CMAQ evaluation results for simu-

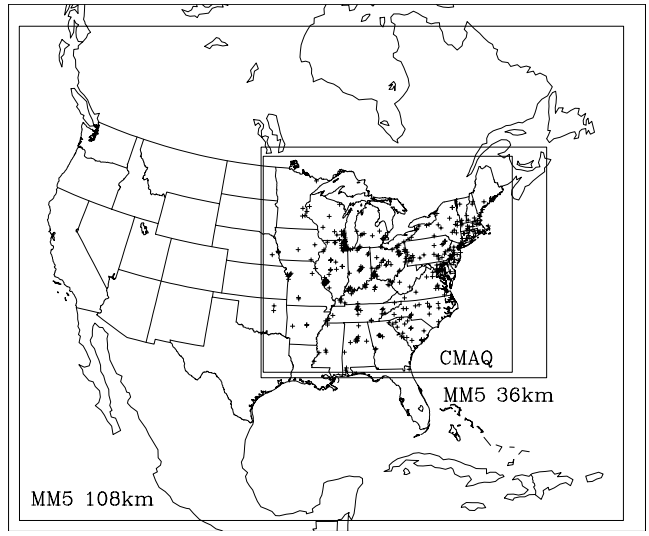

Figure 1. Map showing the 108- and 36-km MM5 modeling domains, the CMAQ modeling domain, and the locations of 428 O_3 monitors (pluses) used to calculate spatial averages over the CMAQ modeling domain.

Table 2. Atmospheric CO_2 Abundances for the A2 Scenario and the Temperature Response of the GISS-GCM and MM5 Models Over All Nonwater Grid Cells for the 36-km CMAQ Modeling Domain Depicted in Figure 1 for the 2020s, 2050s, and 2080s Relative to the 1990s[a]

	Global CO_2 Abundances, ppm	GISS-GCM Temperature Change	MM5 Temperature Change
1990s	353		
2020s	417	+0.8°C	+1.0°C
2050s	532	+1.9°C	+2.7°C
2080s	698	+4.3°C	+5.8°C

[a]Data are from *IPCC* [2001].

lating O_3 concentrations under present-day climate conditions have been presented by *Hogrefe et al.* [2003a, 2003b, 2004]. For the time period 1993–1997 it was found that the global climate model (GCM)/MM5/CMAQ modeling system used in the current study captured interannual and synoptic-scale O_3 variability observed in the current climate. The correlation coefficient between the observed and predicted summertime average 8-hour daily maximum ozone concentrations at all 428 stations for the time period 1993–1997 was 0.63, while the bias was 4 ppb, and the root mean square error was 7 ppb. For the 97.5th percentile the correlation was 0.66, while the bias was 1 ppb, and the root mean square error was 8 ppb [*Hogrefe et al.*, 2004]. The distribution of the frequency and duration of extreme O_3 events was reproduced, with 65/61% of all observed/predicted high 8-hour O_3 events lasting one day, 22/24% of all observed/predicted high 8-hour O_3 events lasting two days, and 13/15% of all observed/predicted high 8-hour O_3 events lasting longer than two days [*Hogrefe et al.*, 2004]. The application of a synoptic map typing procedure revealed that the GCM/MM5/CMAQ system simulated the mean O_3 concentrations associated with several frequent pressure patterns well, indicating that both the mean emission patterns and the effects of synoptic-scale meteorology on O_3 concentrations are well represented in the modeling system used in the current study [*Hogrefe et al.*, 2004].

[9] For the simulations intended to investigate the role of regional climate change in the absence of changes in global tropospheric composition, time-invariant climatological profiles for O_3 and its precursors reflecting present-day clean air concentrations were used as boundary conditions [*Byun and Ching*, 1999]. Table 3 shows these boundary conditions for three of the 16 model layers for selected species. These boundary conditions are distributed with CMAQ, are intended to represent relatively clean air conditions in the eastern half of the United States, and have been formulated from available measurements and results obtained from modeling studies [*Byun and Ching*, 1999]. Since the CMAQ simulations presented in this study are performed for the eastern United States, the choice of these profiles seems justified in the absence of more detailed observations or global chemistry simulations. However, the impact of the choice of boundary conditions on regional-scale ozone simulations is the subject of several ongoing studies such as the ICAP project (http://www.cep.unc.edu/empd/projects/ICAP/index.shtml). The top of the model was at 100 mb, and CMAQ makes a zero-flux assumption for the top boundary; that is, no top boundary concentrations are specified. Therefore the model setup in this study was not designed to simulate stratospheric ozone influx.

[10] For the sensitivity simulations aimed at estimating the role of changes in global atmospheric composition, no simulations for the 2050 A2 scenario performed by a global chemistry model utilizing the same GISS-GCM climate fields driving the MM5 simulation were available to the authors. Therefore these changes were approximated by changing the CMAQ boundary conditions according to values reported in previous studies. For O_3 the boundary conditions for the regional model were increased proportionally to the global average tropospheric column O_3 abundances reported by *Prather and Ehhalt* [2001] for the A2 scenario in 2050. Specifically, all values in the climatological vertical O_3 profiles used as boundary conditions were increased by 30%. This increase is consistent with the average increase in tropospheric O_3 column from 34 to 44.2 Dobson units for the 2050 A2 scenario reported by *Prather and Ehhalt* [2001] that was derived by applying multiple global chemical transport models to simulate the effect of the SRES global emission scenarios in the absence of climate change. While it is likely that changes are not globally uniform and higher in northern midlatitudes, such specific information was not available in a manner consistent with the GISS-GCM climate fields. Changes in boundary conditions for nitrogen species and VOC were determined by scaling the present-day profiles (Table 3) with the NO_x and VOC growth factors of the SRES gridded emissions for the A2 scenario for the OECD90 region shown in Table 1 [*IPCC*, 2000]. This approach assumes that as a first-order approximation, emissions in the western United States and Canada (for which those growth factors are valid) have the largest effect on the boundary conditions for these species for the eastern United States. This assumption is likely to be violated for upper model layers and species with longer lifetimes such as upper tropospheric peroxyacetyl nitrate. A more accurate description of future boundary conditions that takes into account the effect of global emission changes on atmospheric concentrations of nitrogen and VOC species as well as the nonlinear relationship between emission rates and atmospheric concentrations would have required a simulation with a global chemistry model utilizing the GISS-GCM global climate fields for the A2 scenario; such a simulation was not available to the authors. It also should be pointed

Table 3. Time-Invariant Climatological Profiles for O_3 and Selected Species Used as Standard Boundary Conditions for the CMAQ Simulations[a]

	Layer 1 (Midpoint 35 m)	Layer 12 (Midpoint 3,340 m)	Layer 16 (Midpoint 11,500 m)
HCHO, ppt	400	280	50
NO, ppt	83	25	0
PAN,[b] ppt	150	50	15
NO_2, ppt	170	50	0
HNO_3, ppb	0.5	0.38	0.1
O_3, ppb	35	54	70
H_2O_2, ppb	2	1.5	0.2
CO, ppb	80	74	50

[a]Data are from *Byun and Ching* [1999].
[b]PAN is peroxyacetyl nitrate.

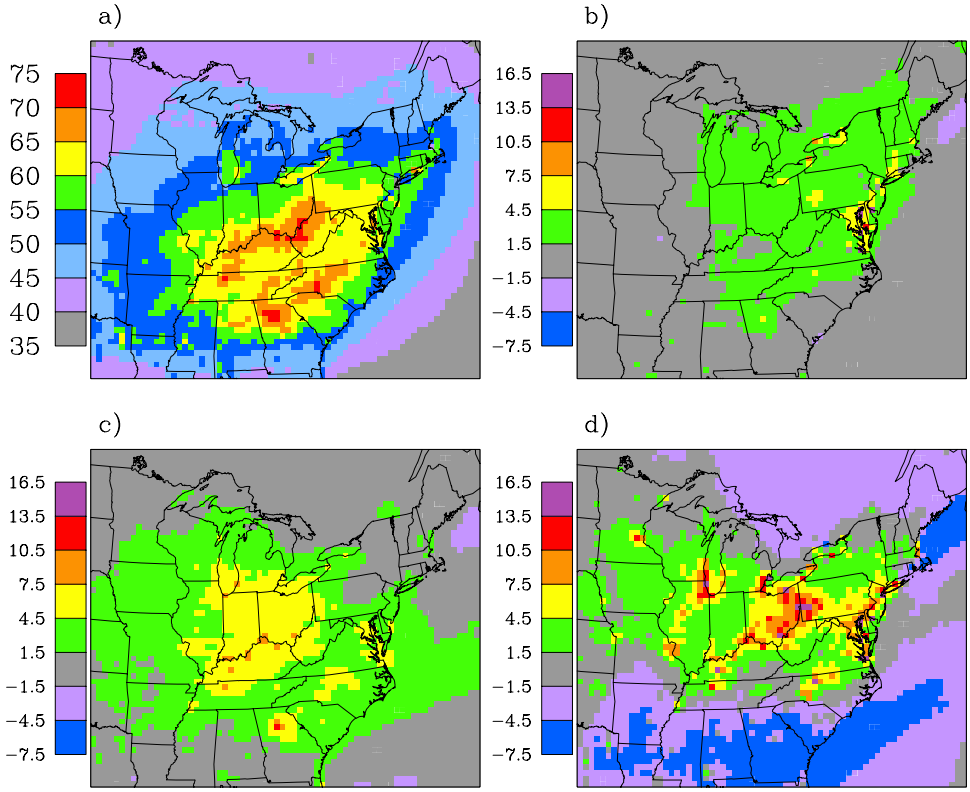

Figure 2. (a) Summertime average daily maximum 8-hour O_3 concentrations for the 1990s and changes in summertime average daily maximum 8-hour O_3 concentrations for the (b) 2020s, (c) 2050s, and (d) 2080s A2 scenario simulations relative to the 1990s, in parts per billion. Five consecutive summer seasons were simulated in each decade.

out that this approach neglects the effect of climate change outside the domain on the chemical composition of the global atmosphere (e.g., through changes in reaction rates, water vapor, transport, and biogenic emissions). To consider these effects, it would be necessary to apply a coupled global/regional climate and chemistry model.

3. Results and Discussion

3.1. Changes in O_3 Due to Regional Climate Change

[11] Figure 2 depicts spatial maps of the average daily maximum 8-hour O_3 concentrations for the 1990s and the increase from these concentrations for the simulations with the A2 climate for the 2020s, 2050s, and 2080s. In these simulations, anthropogenic emissions and boundary conditions were fixed at the levels used for the 1990s, while the calculation of biogenic emissions took into account the temperature and radiation fields for the future climate. For the 2020s, increases in summertime average daily maximum 8-hour O_3 concentrations range from 0 to 8 ppb. The largest increases of 4–8 ppb are predicted for the urban corridor from Washington, D. C., to Massachusetts, while O_3 changes are small for the southern and western portion of the modeling domain. Predicted changes in average summertime daily maximum 8-hour O_3 concentrations for the 2050s are similar in magnitude but occur over a larger area compared to those in the 2020s. In contrast to the 2020s the largest O_3 increase of 4–8 ppb is predicted for the Midwest and the southeastern United States. For the 2080s, predicted O_3 increases exceed 7 ppb for the entire urban corridor from Washington, D. C., to New York City and for the Ohio River Valley. However, summertime average 8-hour daily maximum O_3 concentrations are predicted to decrease for the southern and northern thirds of the modeling domain. Analysis of model results suggests that this O_3 decrease is caused by a sharp increase in convective activity along with increased mixed layer heights predicted by the regional climate model for these regions (B. Lynn, personal communication, 2004). When the increases of summertime average daily maximum 8-hour O_3 concentrations are spatially averaged over the locations of the population-oriented O_3 monitors depicted in Figure 1, the increases are 2.7, 4.2, and 5.0 ppb for the 2020s, 2050s, and 2080s, respectively.

[12] In all decades the largest increases of summertime average daily maximum 8-hour O_3 concentrations typically occur away from the domain boundaries, often in regions of high emissions. Additional analysis shows that there is no strong correlation between the spatial patterns depicted in Figures 2b–2d and corresponding patterns for changes in summertime values of any one of several meteorological variables such as surface temperature, wind speed, and mixed layer height. For example, the regions displaying the largest changes in summertime average daily maximum temperature are not necessarily the same regions that show the largest increases of summertime average daily maximum 8-hour O_3. This exemplifies the complex and nonlinear interactions of

Table 4. Parameters of the Predicted Cumulative Distribution Functions of Domain-Wide 8-hour Daily Maximum Ozone Concentrations for Five Summers Each in the 1990s, 2020s, 2050s, and 2080s[a]

	Observations 1990s	CMAQ 1990s	CMAQ 2020s	CMAQ 2050s	CMAQ 2080s
Five-summer temporal and spatial average, ppb	54	58	60	62	63
Mean (lowest/highest), ppb	53/57	56/60	59/61	58/63	57/69
Variance (lowest/highest), ppb^2	289/365	239/287	296/325	304/349	284/427
Median (lowest/highest), ppb	51/56	54/58	57/59	57/62	55/68
2.5th percentile (lowest/highest), ppb	22/24	30/32	30/33	29/33	31/36
25th percentile (lowest/highest), ppb	40/43	44/47	46/48	45/49	44/54
75th percentile (lowest/highest), ppb	64/69	66/71	70/72	70/76	69/83
97.5th percentile (lowest/highest), ppb	90/97	90/96	97/101	96/102	94/113
Variance of five summertime median values, ppb^2	2.5	2.2	0.7	3.0	23.8

[a]Results for observations for the 1990s are also shown for comparison. Each distribution was derived by considering one value per day per station location (see Figure 1) for June–August for each of the five summers simulated per decade. For each decade the lowest and highest values of a given quantity provide a measure of interannual variability for that quantity. Note that the lowest or highest values for different quantities within the same decade do not necessarily occur in the same year. For example, the highest 2.5th percentile for the 1990s could occur in 1995, but the highest median for the 1990s could occur in 1993.

chemical transformations and atmospheric transport that govern O_3 concentrations. It should also be reiterated that unchanged boundary conditions were used for this set of simulations. The issue of changing boundary conditions to approximate increasing tropospheric background conditions is addressed in section 3.3.

[13] While Figure 2 illustrates the changes in summertime average daily maximum 8-hour O_3 concentrations, it is also important to investigate changes in other aspects of predicted daily maximum 8-hour O_3 concentrations by comparing its cumulative distribution functions under the current and future climate scenarios. To this end, Table 4 lists various aspects of the five summer distributions derived from the domain-wide predictions of daily maximum 8-hour O_3 concentrations for the 1990s, 2020s, 2050s, and 2080s. Specifically, each summer distribution was derived by considering one value per day per station location (see Figure 1) for June–August for one of the five summers simulated per decade. By constructing different distributions for each summer, changes across the decades can be compared to interannual variations within each decade. It can be seen that there is little change in the low end of the distributions, while there is a 1- to 10-ppb increase in the highest summer season mean and median values and a 5- to 17-ppb increase in the highest summer season 97.5th percentile values. Both the intraseasonal variability (as determined by the variance of each individual one-summer distribution function) and the interannual variability (as determined by the variance of the five summer season median values predicted for each five summer periods) show an increase. Furthermore, additional analysis indicates that there is an increase in the fourth highest summertime daily maximum 8-hour O_3 concentration of 5.0, 6.4, and 8.2 ppb for the 2020s, 2050s, and 2080s, respectively, when spatially averaged over the locations of the O_3 monitors depicted in Figure 1. It should be noted that the large increase in interannual variability for the 2080s is mostly caused by a single, anomalously hot summer season in 2086. While there is no reason to discount this result, it implies that the simulations of additional summers would be desirable for all future decades to decrease the influence of such extreme summers on multisummer averages.

[14] Because the U.S. national ambient air quality standard (NAAQS) for 8-hour O_3 concentrations is set at 84 ppb, model-predicted exceedances of this threshold are of particular importance when assessing the effect of climate change on O_3 air quality. To analyze changes in the frequency and duration of extreme O_3 events, the number of days for which the predicted daily maximum 8-hour O_3 concentrations exceeded 84 ppb was determined at the locations of the O_3 monitors shown in Figure 1, and for each such event the number of consecutive days for which these conditions persisted was tracked. The results of this analysis are presented in Figures 3a–3b. Figure 3a shows the total number of days with daily maximum 8-hour O_3 concentrations exceeding 84 ppb for the 1990s, 2020s, 2050s, and 2080s simulations, grouped by the number of consecutive days on which this concentration was exceeded. The total number of exceedance days increased from ~20,000 in the 1990s to ~26,000 in the 2020s, ~33,000 in the 2050s, and ~35,000 in the 2080s, i.e., by roughly 75% by the 2080s.

[15] Spatial maps of the number of additional 8-hour O_3 exceedance days compared to the 1990s show up to 10 additional exceedance days per summer along the eastern seaboard and along the Ohio River Valley for the 2050s and 2080s (not shown). *Fiore et al.* [2002b] determined the increase in O_3 exceedance days with constant climate and changed A1 emissions for 2030 (A1 is a scenario developed by the Intergovernmental Panel on Climate Change). Their results showed an increase in the number of grid square days exceeding 70 ppb of ~70% relative to 1995 [*Fiore et al.*, 2002b]. This number is comparable to the estimate of the effects of regional climate change for the 2050s A2 climate change scenario presented in this study.

[16] To highlight changes in the persistence of extreme O_3 events, Figure 3b presents normalized frequencies of occurrence of pollution episodes of different length. Figure 3b illustrates that for the 1990s, 60% of all high-O_3 events lasted only for a single day, while for the 2080s, more than 50% of all O_3 events lasted for at least 2 days. Thus Figures 3a–3b illustrate that both the number of exceedances and the duration of extreme pollution conditions are predicted to increase in the future regional climate. In investigations of whether multiday ozone exceedance events contribute disproportionately to health effects, results have varied depending on whether study subjects were exposed to high ozone concentrations in controlled environmental chamber studies [*Farrell et al.*, 1979; *Folinsbee*

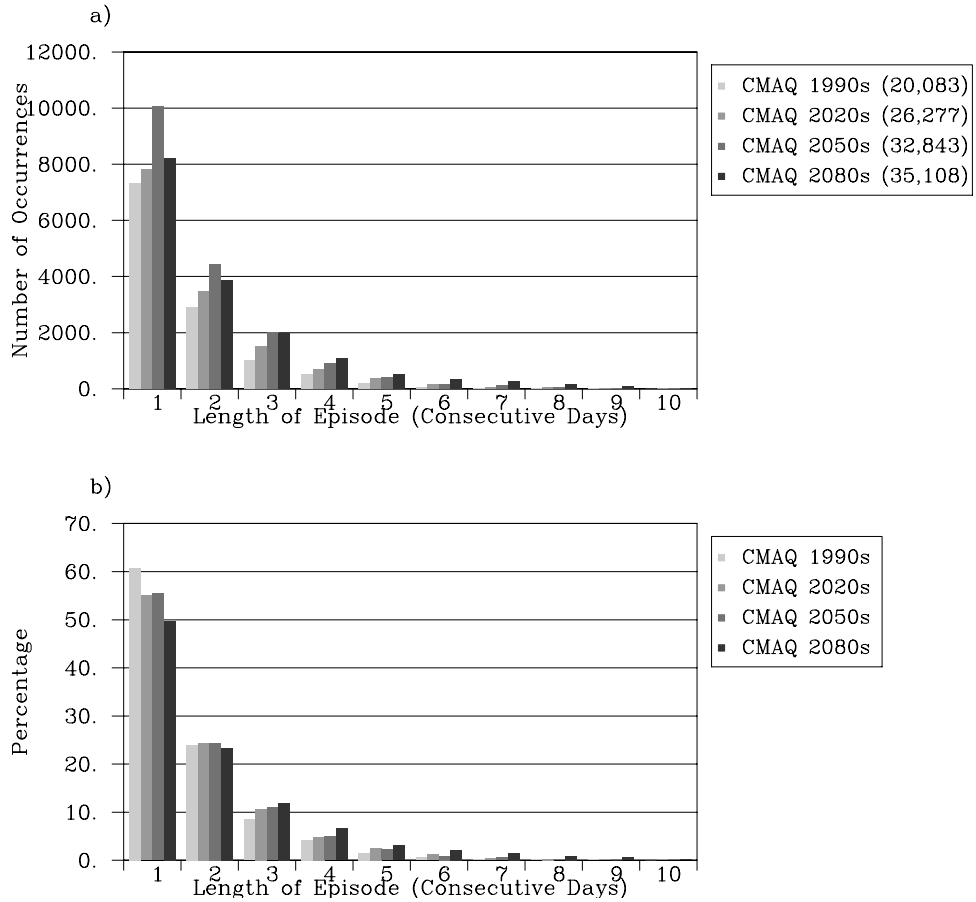

Figure 3. Frequency and duration of extreme ozone events defined as the predicted daily maximum 8-hour O_3 concentration exceeding 84 ppb at the locations of the O_3 monitors shown in Figure 1. (a) Total number of days with daily maximum 8-hour O_3 concentrations exceeding 84 ppb for the 1990s, 2020s, 2050s, and 2080s simulations, grouped by the number of consecutive days on which this concentration was exceeded. The total number of exceedance days for each decade is shown in the legend. (b) Normalized frequencies of occurrence of pollution episodes of different length.

et al., 1980; *Frank et al.*, 2001] versus exposures to more moderate ozone concentrations under ambient environmental conditions [*Spektor et al.*, 1991]. The environmental chamber studies suggest that during multiday (up to 5 days) ozone exposures, there is an initial period (on days 2–4) during which ozone-induced adverse respiratory health effects are cumulative and exceed single-day effects. In most such studies, however, adverse effects were attenuated after 3–5 days' exposure, perhaps due to adaptation. Under ambient summer ozone concentrations, multiple days' exposure among a cohort of healthy, active children show a carryover of adverse effects from prior exposure, with larger effects than those produced by a single day's exposure and no attenuation due to adaptation [*Spektor et al.*, 1991]. Therefore the findings presented above have potentially important implications for population health, especially among active children. In summary, the CMAQ simulations of O_3 concentrations utilizing the 2020s, 2050s, and 2080s A2 regional climate fields from the GISS-MM5 simulations (Lynn et al., submitted manuscript, 2004) show an increase in summertime average daily maximum 8-hour O_3 concentrations, interannual variability of median O_3 values, and an increase in the frequency and duration of extreme O_3 events over the eastern United States in the absence of changes in anthropogenic emissions and boundary conditions.

3.2. Contribution of Biogenic Emissions to Increased O_3 Concentrations

[17] Lynn et al. (submitted manuscript, 2004) showed that the MM5 simulations used as input to the CMAQ simulations performed in this study predict an increase of average summertime daily maximum temperatures of 1.5°–3.5°C for most regions in the modeling domain for the 2050s A2 scenario compared to the 1990s. *Constable et al.* [1999] reported that a mean temperature increase of 6°C from a global circulation model simulation with doubled CO_2 emissions resulted in an increase in isoprene emissions between 40 and 90%. To estimate the first-order contribution of changed biogenic emissions on the ozone changes discussed in section 3.1, a set of sensitivity simulations was performed. In these sensitivity simulations an attempt was made to decouple the increase of biogenic emissions due to rising temperatures from other effects of climate change for the 2050s.

[18] In a first step the summertime total biogenic emissions for the five summers in the 1990s and 2050s

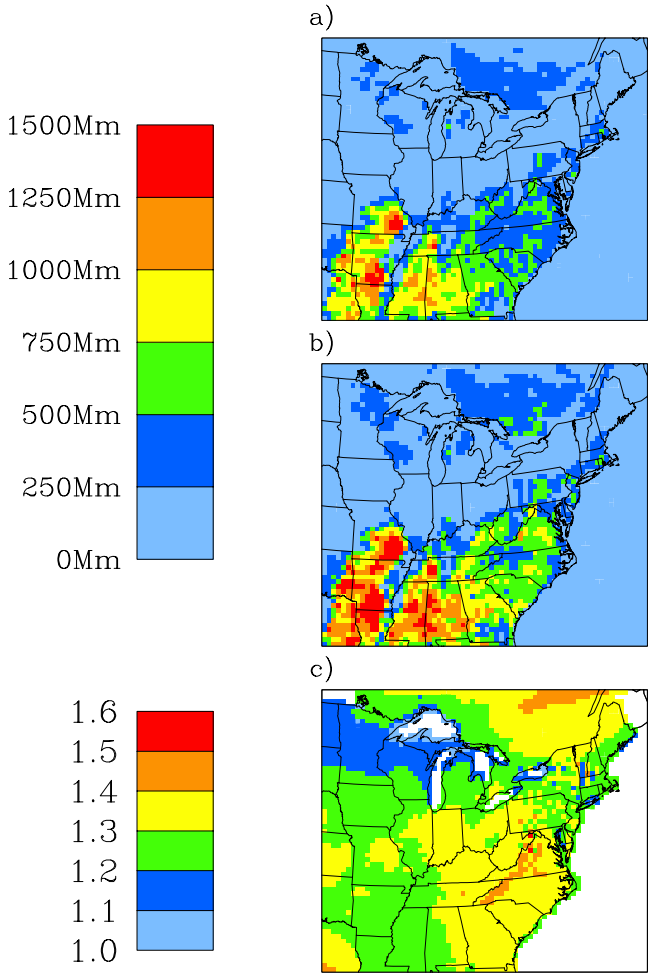

Figure 4. Summertime total biogenic isoprene emissions from biogenic emissions inventory system, version 2 (BEIS2) resulting from the temperature and radiation fields of the (a) 1990s and (b) 2050s MM5 regional climate simulations, in megamoles. (c) Ratio of Figures 4a and 4b.

were calculated for each grid cell using the 1990s and 2050s MM5 temperature and radiation fields. These summertime averages were then used to determine a scaling ratio for summertime total biogenic emission due to climate change for each grid cell. Maps of summertime total isoprene emissions for the 1990s and 2050s as well as the scaling ratio are shown in Figures 4a–4c. Isoprene emissions are highest in the southern part of the modeling domain. The map of the scaling ratio indicates that summertime total isoprene emissions were between 10 and 50% higher for the 2050s climate compared to the 1990s climate. The same procedure was applied to determine scaling ratios for other temperature-dependent biogenic VOC and NO emissions. The scaling ratios were then used to perform hypothetical sensitivity simulations in which the change of ozone stemming from changed biogenic emissions was decoupled from that stemming from changes in climate. It should be noted that these simulations are hypothetical because both effects cannot be isolated in reality. Specifically, we performed simulations with 1993–1997 climate and 1993–1997 hourly biogenic emissions scaled up to match 2050s summertime total biogenic emissions and with 2053–2057 climate and 2053–2057 hourly biogenic emissions scaled down to match 1990s summertime total biogenic emissions. Together with the coupled climate/biogenic emission simulations for the 1990s and 2050s presented in section 3.1, this set of simulations can be used to investigate the ozone changes that occur when climate changes but summertime total biogenic emissions are held constant or vice versa. In addition, the factor separation approach introduced by *Stein and Alpert* [1993] allows the detection of ozone changes that only occur when both climate and biogenic emissions change, the so-called synergistic effect. Results from these simulations are shown in Figures 5a–5c and indicate that increased biogenic emissions alone add 1–3 ppb to

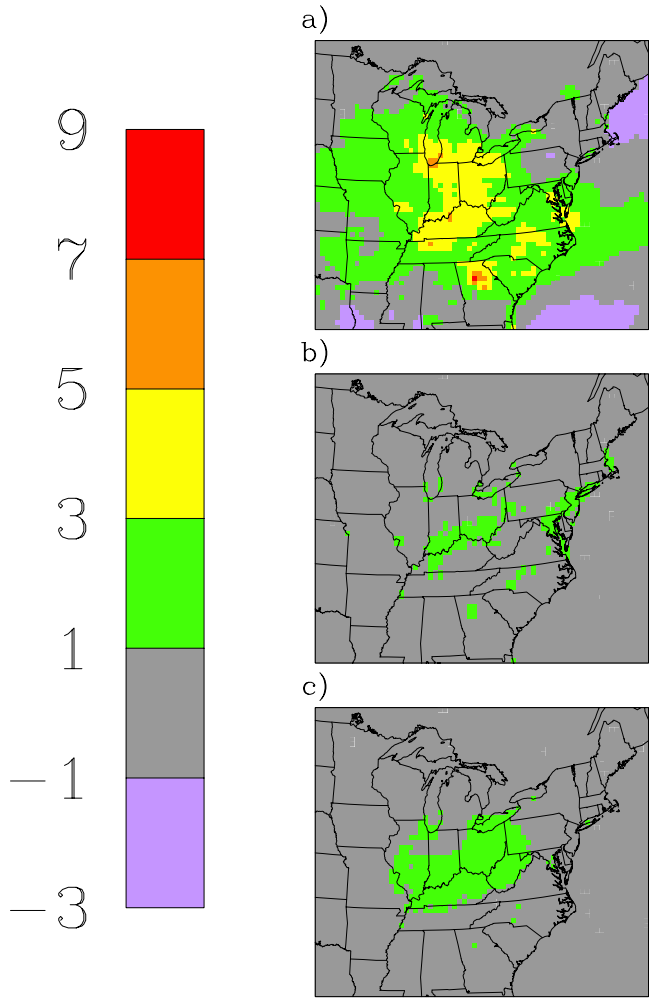

Figure 5. Increase in summertime average daily maximum 8-hour O_3 concentrations from the 1990s to the 2050s (a) as a result of climate change without considering the effects of increased biogenic emissions, (b) as a result of increased biogenic emissions without considering other effects of climate change, and (c) as a result of the interaction between the two effects, in parts per billion. Total change in ozone concentrations resulting from a change in both factors is equal to the sum of all three panels.

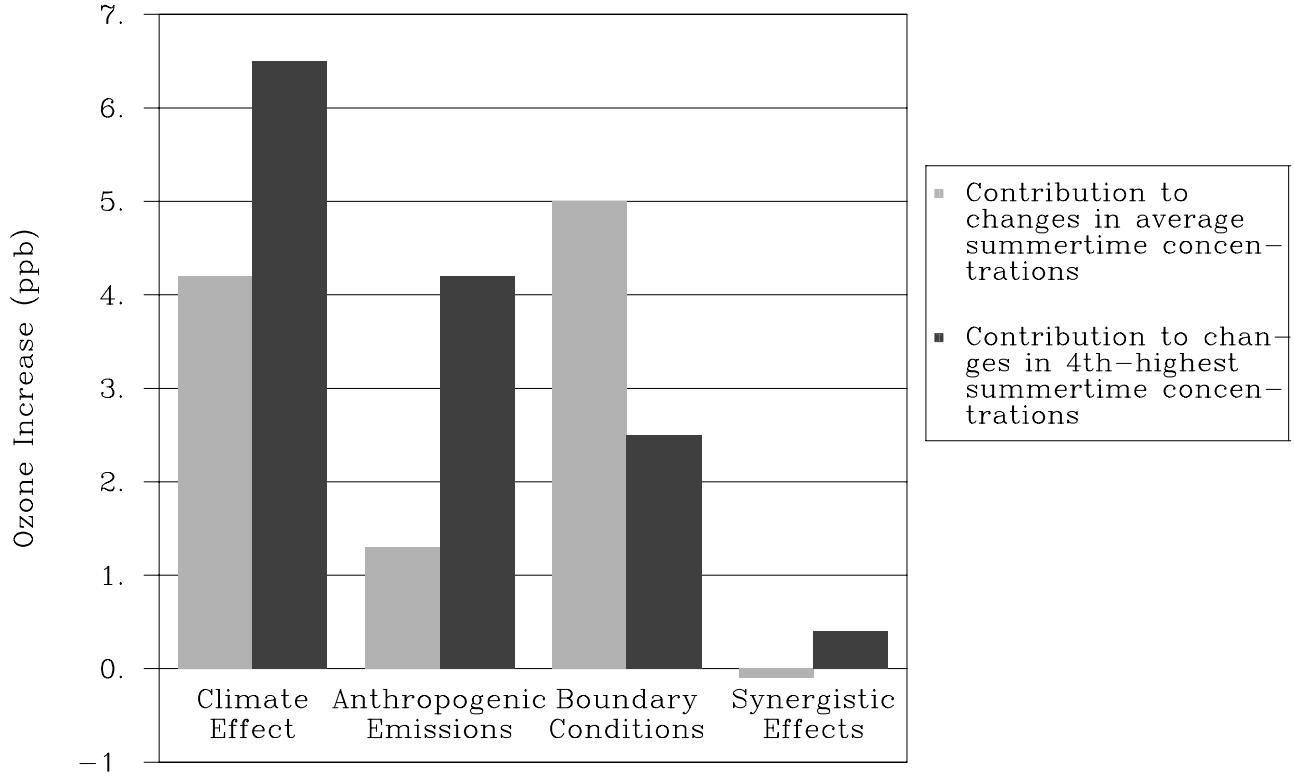

Figure 6. Spatially averaged contribution of climate-induced changes, anthropogenic emission-induced changes, and boundary condition-induced changes to changes in summertime average daily maximum 8-hour O_3 concentrations and changes in the fourth highest summertime daily maximum 8-hour O_3 concentration from the 1990s to the 2050s.

summertime average daily maximum 8-hour O_3 concentrations in the Midwest and along the eastern seaboard, while climate effects other than changes in biogenic emissions increase average daily maximum 8-hour O_3 concentrations by 3–5 ppb in the Great Lakes region and lead to small O_3 decreases in the south and parts of the northeast. Synergistic effects between the two forcings as defined by *Stein and Alpert* [1993] account for an increase of 1–3 ppb for the center of the modeling domain (Figure 5c). On a spatial average basis, increased summertime total biogenic emissions and synergistic effects between climate change and increased emissions account for about half of the overall increase in summertime average daily maximum 8-hour O_3 concentrations shown in Figure 2 for the 2050s.

3.3. Relative Impact of Changes in Anthropogenic Emissions Versus Changes in Regional Climate

[19] The analysis presented in sections 3.1–3.2 focused on determining the effects of climate change on summertime O_3 concentrations over the eastern United States in the absence of changes in anthropogenic emissions within the modeling domain or changes in boundary conditions approximating changes in global atmospheric composition as discussed in section 2.3. Previous studies have investigated the effects of increasing global and regional emissions on O_3 air quality using global atmospheric chemistry models [*Prather and Ehhalt*, 2001; *Fiore et al.*, 2002b; *Prather et al.*, 2003] in the absence of climate change. While a fully coupled, multiscale dynamics-chemistry model would be necessary to study all interactions between climate and air quality on both regional and global scales, the regional-scale model system described in this study can be used to compare the effects of climate change on air quality presented in sections 3.1–3.2 to the effects of increases in anthropogenic emissions within the modeling domain and the approximated effects of changes in global atmospheric composition through the specification of altered boundary conditions for the regional model as described in section 2.3.

[20] As in section 3.2, the sensitivity simulations were performed for the time periods from 1993 to 1997 and 2053 to 2057. A complete set of 40 sensitivity simulations was performed for all possible combinations of current and future climate, current and future anthropogenic emissions within the modeling domain, and current and future chemical boundary conditions to assess the individual and synergistic effects of changes in these factors. Subsequently, we analyzed the contribution of the above-mentioned factors to both average summertime daily maximum 8-hour O_3 concentrations and to extreme O_3 events that are most relevant from a U.S. regulatory perspective.

[21] To compare the contribution of the three factors to changes in summertime average daily maximum 8-hour O_3 concentrations as well as the fourth highest summertime daily maximum 8-hour O_3 concentration that is of

relevance to the NAAQS, these contributions were calculated and averaged at the sites of the O_3 monitors depicted in Figure 1. Figure 6 shows a bar chart of the contribution of each factor and the synergistic effect as defined by *Stein and Alpert* [1993] to changes in summertime average daily maximum 8-hour O_3 concentrations (light shading) and to changes in the fourth highest summertime daily maximum 8-hour O_3 concentration in the 2050s A2 scenario simulation (dark shading).

[22] Figure 6 indicates that changed boundary conditions as described in section 2.3 are the largest contributor (5.0 ppb or 48% of the total increase) to changes in summertime average daily maximum 8-hour O_3 concentration in the 2050s A2 scenario simulation from the 1990s base simulation, followed by the effects of climate change (4.2 ppb or 40% of the total increase) and the effects of increased anthropogenic emissions within the modeling domain (1.3 ppb or 12% of the total increase). The sum of all interaction between these effects is negligible. For comparison, *Fiore et al.* [2002b] show an increase in mean summertime afternoon surface O_3 concentrations of 4 ppb for the United States under the 2030 A1 emission scenario relative to 1995 with constant climate. Neglecting the effect of climate change not considered by their study, the increase in average summertime daily maximum 8-hour surface O_3 concentrations predicted in this study for the 2050 A2 scenario is 6.3 ppb (5.0-ppb boundary effect and 1.3-ppb U.S. anthropogenic emission effect). This larger increase is consistent with the larger NO_x emissions in the 2050 A2 scenario (+30/+126% OECD90/global) compared to the 2030 A1 scenario (−20/+80% OECD90/global).

[23] In a different study, *Prather et al.* [2003] reported near-surface O_3 increases of 20 ppb and larger for the 2100 A2 scenario simulated by 10 global chemical transport models as a result of rising emissions in the absence of climate change. *Prather et al.* [2003] also proposed to scale these near-surface O_3 changes with the changes in total tropospheric column O_3 reported by *Prather and Ehhalt* [2001] to estimate changes in near-surface O_3 for different scenarios and decades. When following this methodology, one would obtain an estimated increase of near-surface summer average O_3 concentrations of ∼10 ppb for the 2050 A2 emission scenario in the absence of climate change, larger than the 6.5-ppb nonclimate increase reported in this study. In the present simulation, increases of this magnitude are only seen near the domain boundary (where boundary conditions had been increased by 30% or 10 ppb near the surface) but are smaller for most of the modeling domain. This could be due to an underestimation of the magnitude of changes in background O_3, VOC, and nitrogen species using the methodology described in section 2.3 compared to the global chemistry simulations analyzed by *Prather and Ehhalt* [2001] and *Prather et al.* [2003]. Another reason for the difference could be that the archived changes in the total tropospheric column O_3 might not be an adequate tool to estimate changes in near-surface O_3 because of the vertical gradients and intermodel variability of the tropospheric O_3 changes predicted by the various global chemical transport models used by *Prather and Ehhalt* [2001].

[24] The ranking of the factors changes dramatically when comparing the fourth highest daily maximum 8-hour O_3 concentration predicted in the 2050s A2 scenario simulation to that predicted in the 1990s base simulation (Figure 6). Assessing changes in this extreme O_3 concentration is important because of its relevance to the U.S. NAAQS for 8-hour O_3 concentrations. For this extreme O_3 concentration the effects of climate change account for an increase of 6.5 ppb (48% of the total increase), followed by the effect of increased anthropogenic emissions (4.2 ppb or 31% of the total increase) and increased boundary conditions (2.5 ppb or 18% of the total increase). The sum of all interaction between these effects is 0.4 ppb or 3% of the total increase. The reduced importance of changed boundary conditions for changes in the fourth highest daily maximum 8-hour O_3 concentration is consistent with previous studies that showed that high ozone concentrations in the eastern United States often occur under synoptic conditions characterized by slow-moving high-pressure systems, clear skies, and lower wind speeds [*Gaza*, 1998; *Vukovich*, 1995]. Such conditions tend to reduce the impacts of inflow from the model boundaries. Figures 7a–7d present maps of the fourth highest summertime daily maximum 8-hour ozone concentration for the 1990s (Figure 7a), the contributions of climate change (including increased biogenic emissions) (Figure 7b), anthropogenic emission change (Figure 7c), and changed boundary conditions (Figure 7d) to the fourth highest summertime daily maximum 8-hour O_3 concentration that occurs in a simulation for which all factors are changed to their 2050s A2 value. It can be seen that the effect of climate change on O_3 is largest along the east coast and in the Midwest with changes of 7–11 ppb. The effect of increased anthropogenic emissions is largest in the southeast, consistent with previous findings that O_3 production in this region is very sensitive to the amount of anthropogenic NO_x emissions because of the abundance of biogenic hydrocarbon emissions [*Tao et al.*, 2003]. Finally, the effect of boundary conditions is largest toward the northwestern corner of the modeling domain (11 ppb), while it is only 1–3 ppb for most of the modeling domain. In summary, while previous studies have pointed out the potentially important contribution of growing global emissions and intercontinental transport to O_3 air quality in the United States for future decades, the results presented in this section imply that the effects of a changing climate may be of at least equal importance when planning for the future attainment of the NAAQS. In future studies, fully coupled, multiscale dynamics-chemistry models should be applied for a range of climate and emission scenarios to investigate the relative impacts of the different factors on regional air quality in a comprehensive manner.

4. Conclusions

[25] This paper described the application of a one-way coupled global/regional modeling system used to simulate O_3 air quality in future decades over the eastern United States. The CMAQ simulations of O_3 concentrations utilizing the regional climate fields for the A2 emission

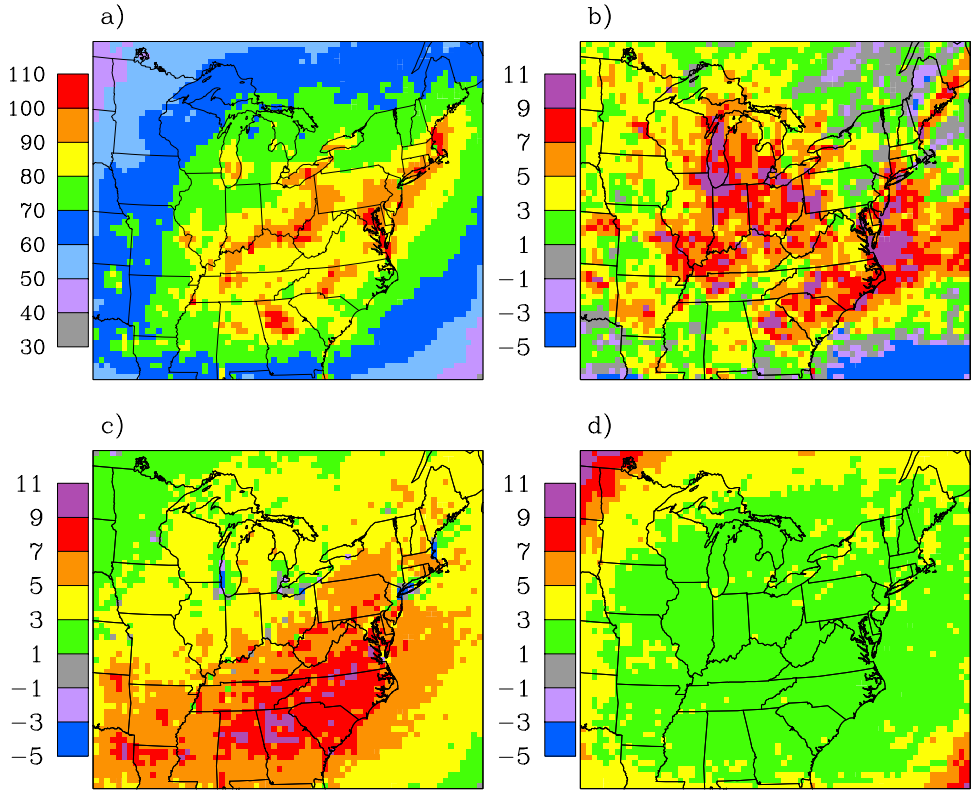

Figure 7. (a) Average fourth highest summertime daily maximum 8-hour O_3 concentration for the 1990s, (b) changes in the average summertime fourth highest daily maximum 8-hour O_3 concentrations from the 1990s to the 2050s as a result of climate change, (c) changes in the average summertime fourth highest daily maximum 8-hour O_3 concentrations from the 1990s to the 2050s as a result of increased anthropogenic NO_x/VOC emissions of 30/8% within the modeling domain, and (d) changes in the average summertime fourth highest daily maximum 8-hour O_3 concentrations from the 1990s to the 2050s as a result of increased boundary conditions as described in section 2.3, in parts per billion.

scenario for the 2020s, 2050s, and 2080s show an increase in spatially and temporally averaged summertime daily maximum 8-hour O_3 concentrations of 2.7, 4.2, and 5.0 ppb, respectively, in the absence of changes in anthropogenic emissions and boundary conditions. For the 2050s it was determined that about half of this overall increase in summertime average daily maximum 8-hour O_3 concentrations is caused directly or indirectly by the change in biogenic emissions. Furthermore, an increase of the interannual variability of median O_3 values and an increase in the frequency and duration of extreme O_3 events over the eastern United States is predicted, although simulations over longer periods in future decades would be desirable to further dampen the effect of individual extreme summers on these results.

[26] Through additional sensitivity simulations for the 2050s the relative impact of changes in regional climate, anthropogenic emission within the modeling domain, and changes in global atmospheric compositions as approximated by changed boundary conditions for the regional-scale model was investigated. Relative to the 1990s, changed boundary conditions are the largest contributor to changes in predicted summertime average daily maximum 8-hour O_3 concentrations, followed by the effects of regional climate change and the effects of increased anthropogenic emissions within the modeling domain. However, when changes in the fourth highest summertime daily maximum 8-hour O_3 concentration are considered, changes in regional climate are the most important contributor to simulated concentration changes, followed by the effect of increased anthropogenic emissions and increased boundary conditions. Thus, while previous studies have pointed out the potentially important contribution of growing global emissions and intercontinental transport to O_3 air quality in the United States for future decades, the results presented in this study imply that the effects of a changing climate may be of at least equal importance when planning for the future attainment of regional-scale air quality standards such as the U.S. NAAQS. However, it should be noted that future studies utilizing fully coupled, multiscale dynamics-chemistry models are needed to account for all interactions between emissions, climate, and air quality on both regional and global scales and to investigate the relative impacts of different factors on regional air quality in a comprehensive manner for a range of climate and emission scenarios.

[27] **Acknowledgments.** This work is supported by the U.S. Environmental Protection Agency under STAR grant R-82873301. Although the research described in this article has been funded in part by the U.S. Environmental Protection Agency, it has not been subjected to the agency's required peer and policy review and therefore does not necessarily reflect the views of the agency, and no official endorsement should be inferred.

References

Aw, J., and M. J. Kleeman (2003), Evaluating the first-order effect of intraannual temperature variability on urban air pollution, *J. Geophys. Res.*, *108*(D12), 4365, doi:10.1029/2002JD002688.

Bell, M., and H. Ellis (2003), Comparison of the 1-hr and 8-hr National Ambient Air Quality Standards for ozone using Models-3, *J. Air Waste Manage. Assoc.*, *53*, 1531–1540.

Berge, E., H.-C. Huang, J. Chang, and T.-H. Liu (2001), A study of the importance of initial conditions for photochemical oxidant modeling, *J. Geophys. Res.*, *106*, 1347–1363.

Betts, A. K. (1986), A new convective adjustment scheme. Part I: Observational and theoretical basis, *Q. J. R. Meteorol. Soc.*, *112*, 677–692.

Brasseur, G. P., J. T. Kiehl, J.-F. Müller, T. Schneider, C. Granier, X. X. Tie, and D. Hauglustaine (1998), Past and future changes in global tropospheric ozone: Impact on radiative forcing, *Geophys. Res. Lett.*, *25*(20), 3807–3810.

Byun, D. W., and J. K. S. Ching (Eds.) (1999), Science algorithms of the EPA Models-3 Community Multiscale Air Quality Model (CMAQ) modeling system, *EPA/600/R-99/030*, U.S. Environ. Prot. Agency, Off. of Res. and Dev., Washington, D. C.

Constable, J. V. H., A. B. Guenther, D. S. Schimel, and R. K. Monson (1999), Modelling changes in VOC emissions in response to climate change in the continental United States, *Global Change Biol.*, *5*, 791–806.

Davies, H. C., and R. E. Turner (1977), Updating prediction models by dynamical relaxation: An examination of the technique, *Q. J. R. Meteorol. Soc.*, *103*, 225–245.

Farrell, B. P., H. D. Kerr, T. J. Kulle, L. R. Sauder, and J. L. Young (1979), Adaptation in human subjects to the effects of inhaled ozone after repeated exposure, *Am. Rev. Respir. Dis.*, *119*(5), 725–730.

Fiore, A. M., D. L. Jacob, I. Bey, R. M. Yantosca, B. D. Field, A. C. Fusco, and J. G. Wilkinson (2002a), Background ozone over the United States in summer: Origin, trend, and contribution to pollution episodes, *J. Geophys. Res.*, *107*(D15), 4275, doi:10.1029/2001JD000982.

Fiore, A. M., D. J. Jacob, B. D. Field, D. G. Streets, S. D. Fernandes, and C. Jang (2002b), Linking ozone pollution and climate change: The case for controlling methane, *Geophys. Res. Lett.*, *29*(19), 1919, doi:10.1029/2002GL015601.

Fiore, A., D. J. Jacob, H. Liu, R. M. Yantosca, T. D. Fairlie, and Q. Li (2003a), Variability in surface ozone background over the United States: Implications for air quality policy, *J. Geophys. Res.*, *108*(D24), 4787, doi:10.1029/2003JD003855.

Fiore, A. M., T. A. Holloway, and M. G. Hastings (2003b), A global perspective on air quality: Intercontinental transport and linkages with climate, *Environ. Manage.*, *69*, 13–22.

Folinsbee, L. J., J. F. Bedi, and S. M. Horvath (1980), Respiratory responses in humans repeatedly exposed to low concentrations of ozone, *Am. Rev. Respir. Dis.*, *121*(3), 431–439.

Frank, R., M. C. Liu, E. W. Spannhake, S. Mlynarek, K. Macri, and G. G. Weinmann (2001), Repetitive ozone exposure of young adults: Evidence of persistent small airway dysfunction, *Am. J. Respir. Crit. Care Med.*, *164*(7), 1253–1260.

Gaza, R. S. (1998), Mesoscale meteorology and high ozone in the northeast United States, *J. Appl. Meteorol.*, *37*, 961–967.

Geron, C. D., A. B. Guenther, and T. E. Pierce (1994), An improved model for estimating emissions of volatile organic compounds from forests in the eastern United States, *J. Geophys. Res.*, *99*, 12,773–12,791.

Gery, M. W., G. Z. Whitten, J. P. Killus, and M. C. Dodge (1989), A photochemical kinetics mechanism for urban and regional-scale computer modeling, *J. Geophys. Res.*, *94*, 12,925–12,956.

Grell, G. A., J. Dudhia, and D. Stauffer (1994), A description of the fifth-generation Penn State/NCAR Mesoscale Model (MM5), in *NCAR Technical Note*, *TN-398 + STR*, 138 pp., Natl. Cent. for Atmos. Res., Boulder, Colo.

Hogrefe, C., et al. (2003a), Modeling the impact of global climate and regional land use change on regional climate and air quality over the northeastern United States, paper presented at 26th International Technical Meeting on Air Pollution Modeling and its Application, N. Atl. Treaty Organ./Com. on the Challenges of Mod. Soc., Istanbul, Turk., May 26–30.

Hogrefe, C., J. Biswas, K. Civerolo, J.-Y. Ku, B. Lynn, J. Rosenthal, K. Knowlton, R. Goldberg, C. Rosenzweig, and P. L. Kinney (2003b), Climate change and ozone air quality over the eastern United States: A modeling study, *Eos Trans. AGU*, *84*(46), Fall Meet. Suppl., Abstract U32A-0027.

Hogrefe, C., J. Biswas, B. Lynn, K. Civerolo, J.-Y. Ku, J. Rosenthal, C. Rosenzweig, R. Goldberg, and P. L. Kinney (2004), Simulating regional-scale ozone climatology over the eastern United States: Model evaluation results, *Atmos. Environ.*, *38*, 2627–2638.

Holloway, T. A., A. M. Fiore, and M. G. Hastings (2003), Intercontinental transport of air pollution: Will emerging science lead to a new hemispheric treaty?, *Environ. Sci. Technol.*, *37*, 4535–4542.

Hong, S.-Y., and H.-L. Pan (1996), Nonlocal boundary layer vertical diffusion in a medium-range forecast model, *Mon. Weather Rev.*, *124*, 2322–2339.

Intergovernmental Panel on Climate Change (IPCC) (2000), *Special Report on Emissions Scenarios*, edited by N. Nacenovic and R. Swart, 612 pp., Cambridge Univ. Press, New York.

Intergovernmental Panel on Climate Change (IPCC) (2001), *Climate Change 2001: The Scientific Basis*, edited by J. T. Houghton et al., 944 pp., Cambridge Univ. Press, New York.

Jacob, D. J., J. A. Logan, and P. P. Murti (1999), Effect of rising Asian emissions on surface ozone in the United States, *Geophys. Res. Lett.*, *26*(14), 2175–2178.

Johnson, C. E., W. J. Collins, D. S. Stevenson, and R. G. Derwent (1999), Relative roles of climate and emissions changes on future tropospheric oxidant concentrations, *J. Geophys. Res.*, *104*, 18,631–18,645.

Johnson, C. E., D. S. Stevenson, W. J. Collins, and R. G. Derwent (2001), Role of climate feedback on methane and ozone studied with a coupled Ocean-Atmosphere-Chemistry model, *Geophys. Res. Lett.*, *28*(9), 1723–1726.

Ku, J.-Y., H. Mao, K. Zhang, K. Civerolo, S. T. Rao, C. R. Philbrick, B. Doddridge, and R. Clark (2001), Numerical investigation of the effects of boundary-layer evolution on the prediction of ozone and the efficacy of emission control options in the northeastern United States, *Environ. Fluid Mech.*, *1*, 209–233.

McCarthy, J. J., O. F. Canziani, N. A. Leary, D. J. Dokken, and K. S. White (Eds.) (2001), *Climate Change 2001: Impacts, Adaptation and Vulnerability*, Cambridge Univ. Press, New York.

Mebust, M. R., B. K. Eder, F. S. Binkowski, and S. J. Roselle (2003), Models-3 Community Multiscale Air Quality (CMAQ) model aerosol component 2: Model evaluation, *J. Geophys. Res.*, *108*(D6), 4184, doi:10.1029/2001JD001410.

Mlawer, E. J., S. J. Taubman, P. D. Brown, M. J. Iacono, and S. A. Clough (1997), Radiative transfer for inhomogeneous atmosphere: RRTM, a validated correlated-k model for the longwave, *J. Geophys. Res.*, *102*, 16,663–16,682.

Pepper, W. J., W. Barbour, A. Sankovski, and B. Braaz (1998), No-policy greenhouse gas emission scenarios: Revisiting IPCC 1992, *Environ. Sci. Policy*, *1*, 289–312.

Prather, M., and D. Ehhalt (2001), Atmospheric chemistry and greenhouse gases, in *Climate Change 2001: The Scientific Basis*, edited by J. T. Houghton et al., chap. 4, pp. 239–287, Cambridge Univ. Press, New York.

Prather, M., et al. (2003), Fresh air in the 21st century?, *Geophys. Res. Lett.*, *30*(2), 1100, doi:10.1029/2002GL016285.

Russell, G. L., J. R. Miller, and D. Rind (1995), A coupled atmosphere-ocean model for transient climate change studies, *Atmos. Ocean*, *33*, 683–730.

Sankovski, A., W. Barbour, and W. Pepper (2000), Quantification of the IS99 emission scenario storylines using the Atmospheric Stabilization Framework (ASF), *Technol. Forecasting Soc. Change*, *63*, 2–3.

Sillman, S., and P. J. Samson (1995), Impact of temperature on oxidant photochemistry in urban, polluted, rural, and remote environments, *J. Geophys. Res.*, *100*, 1497–1508.

Sistla, G., W. Hao, J.-Y. Ku, G. Kallos, K. Zhang, H. Mao, and S. T. Rao (2001), An operational evaluation of two regional-scale ozone air quality modeling systems over the eastern United States, *Bull. Am. Meteorol. Soc.*, *82*, 945–964.

Spektor, D. M., G. D. Thurston, J. Mao, D. He, C. Hayes, and M. Lippmann (1991), Effects of single- and multiday ozone exposures on respiratory function in active normal children, *Environ. Res.*, *55*, 107–122.

Stein, U., and P. Alpert (1993), Factor separation in numerical simulations, *J. Atmos. Sci.*, *50*, 2107–2115.

Tao, Z., S. M. Larson, D. J. Wuebbles, A. Williams, and M. Caughey (2003), A summer simulation of biogenic contribution to ground-level

ozone over the continental United States, *J. Geophys. Res.*, *108*(D14), 4404, doi:10.1029/2002JD002945.

U.S. Environmental Protection Agency (1994), User's guide to Mobile5 (Mobile source emission factor model), *Rep. EPA/AA/TEB/94/01*, Ann Arbor, Mich.

U.S. Environmental Protection Agency (2004), *The Ozone Report: Measuring Progress Through 2003*, *Rep. EPA 454/K-04-001*, Research Triangle Park, N. C.

Vukovich, F. M. (1995), Regional-scale boundary layer ozone variations in the eastern United States and their association with meteorological variations, *Atmos. Environ.*, *29*, 2259–2273.

Wild, O., and H. Akimoto (2001), Intercontinental transport of ozone and its precursors in a three-dimensional global CTM, *J. Geophys. Res.*, *106*, 27,729–27,744.

Williams, E. J., A. Guenther, and F. C. Fehsenfeld (1992), An inventory of nitric oxide emissions from soils in the United States, *J. Geophys. Res.*, *97*, 7511–7519.

Yienger, J. J., M. Galanter, T. A. Holloway, M. H. Phadnis, S. K. Guttikunda, G. R. Carmichael, W. J. Moxim, and H. Levy II (2000), The episodic nature of air pollution transport from Asia to North America, *J. Geophys. Res.*, *105*, 26,931–26,946.

K. Civerolo, C. Hogrefe, and J.-Y. Ku, New York State Department of Environmental Conservation, Bureau of Air Quality Analysis and Research, 625 Broadway, Albany, NY 12233-3259, USA. (chogrefe@dec.state.ny.us)

S. Gaffin and B. Lynn, Center for Climate Systems Research, Columbia Earth Institute of Columbia University, Columbia University, 2880 Broadway, New York, NY 10025, USA.

R. Goldberg and C. Rosenzweig, NASA Goddard Institute for Space Studies, 2880 Broadway, New York, NY 10025, USA.

P. L. Kinney, K. Knowlton, and J. Rosenthal, Mailman School of Public Health, Columbia University, 722 West 168th Street, New York, NY 10032-2603, USA.